Studies on the catalytic decomposition of N_2O on $LnSrFeO_4$ (Ln = La, Pr, Nd, Sm and Gd)

J. Christopher and **C. S. Swamy**
Department of Chemistry, Indian Institute of Technology, Madras 600 036 (India)

(Received September 20, 1990; revised April 4, 1991)

Abstract

Oxides with the composition $LnSrFeO_4$ (Ln = La, Pr, Nd, Sm and Gd) were prepared by ceramic method and characterised by XRD, IR, conductivity and magnetic measurements. The surface of these oxides was characterised by XPS to estimate the valence state of each element and their relative concentrations. Decomposition of N_2O was carried out on these oxides to establish the role of the rare earth on catalytic activity at 50 and 200 torr in the temperature range 420–480 °C. The catalytic activity was correlated to the bulk and surface properties of these oxides.

Introduction

Oxides with perovskite and related structures are emerging as important prototype models for catalytic studies. Reports on oxides having a K_2NiF_4 structure have revealed that these oxides exhibited greater activity compared to the analogous perovskite oxides [1, 2]. The catalytic activity of Co-, Ni-, Cu-, and Zn-containing oxides with a K_2NiF_4 structure has been examined for various reactions [1–6]. However, the catalytic activity of iron-containing oxides with a K_2NiF_4 structure has not received much attention in the literature, although corresponding perovskite oxides are known to be active for various reactions [7].

Ln_2FeO_4 cannot be prepared due to the unfavourable tolerance factor and difficulty in stabilising iron in the divalent state. There are, however reports available wherein iron is stabilised in the trivalent and tetravalent states with K_2NiF_4 structure, such as $LnSrFeO_4$ [8], $LaSrM_{0.5}Fe_{0.5}O_4$ [9] where M = Mg or Zn, and $LaSrLi_{0.5}Fe_{0.5}O_4$ [10]. Although these compounds are known for their interesting solid state properties, no reports are available on their catalytic activity. In the present investigation, an attempt has been made to evaluate the catalytic activity of iron-containing oxides having a K_2NiF_4 structure. The effect of substitution of rare-earth ions on the solid state and catalytic properties has been studied, choosing $LnSrFeO_4$ compounds in which Fe^{3+} is stabilised in the presence of strontium. Decomposition of N_2O was used as a test reaction for the first time to evaluate the catalytic activity of these oxides.

0304-5102/91/$3.50

Experimental

The catalysts used in the present investigation were prepared by the ceramic method by heating Ln_2O_3, $SrCO_3$ and Fe_2O_3 at 1300 °C for 48 h. The formation of a single phase was confirmed by XRD. IR spectra of these compounds were recorded on a Perkin-Elmer infrared spectrometer (Model 1310). Electrical conductivity measurements were carried out in a two-probe cell in the temperature range 30–500 °C. Magnetic measurements were performed in a vibrating sample magnetometer (Model PAR 155) at room temperature by applying a magnetic field of 0–12 kGauss. Surface area of these compounds was determined by BET method employing N_2 as adsorbate at liquid N_2 temperature. The surface of these oxides was examined by XPS using an Escalab Mark II (VG Scientific, U.K.) spectrometer. XP spectra were recorded at room temperature using Al K_α radiation and a base pressure of 5×10^{-8} mbar.

Decomposition of N_2O was carried out in a static recirculatory reactor at two different pressures of N_2O, namely 50 and 200 torr, in the temperature range 400–480 °C. The catalysts were pretreated before each kinetic measurements: (i) evacuation of the catalyst to 10^{-5} torr at 500 °C for 6 h; (ii) soaking the catalyst in oxygen (100 torr) for 12 h at reaction temperature; (iii) mild evacuation for 2 min using rotary pump for removing weakly adsorbed and gas phase oxygen. The pretreated catalysts are found to give reproducible results.

Results and discussion

All the compounds were found to crystallise in tetragonal symmetry. Table 1 presents the structural parameters such as crystal symmetry, lattice parameters, volume of unit cell and tolerance factors. The unit cell parameters calculated in this investigation are in fairly good agreement with those reported for the same systems. As can be seen, the unit cell decreases from La → Gd, indicating lanthanide contraction across the series. The tolerance factors given in Table 1 were calculated using the high spin ionic radius of

TABLE 1

Structural parameters of $LnSrFeO_4$

Compound	Symmetry[a]	Lattice parameters (A°)		t	c/a
		a	c		
$LaSrFeO_4$	T	3.854	12.667	0.9209	3.287
$PrSrFeO_4$	T	3.840	12.588	0.9145	3.279
$NdSrFeO_4$	T	3.832	12.503	0.9131	3.263
$SmSrFeO_4$	T	3.825	12.487	0.9064	3.265
$GdSrFeO_4$	T	3.821	12.434	0.9024	3.254

[a]T = tetragonal.

Fe^{3+} (0.645 Å) which falls in the range reported for the K_2NiF_4 structure [11]. Table 1 also shows a decrease in c/a values from La → Gd. It is known [12] that if the transition metal ion present in oxides having K_2NiF_4 is a Jahn–Teller ion such as Ni^{2+} or Cu^{2+}, then the c/a value will be greater than 3.35. In the present case Fe^{3+} is not a Jahn–Teller ion and hence c/a values are less than 3.35.

Figure 1 shows the IR spectra of $LnSrFeO_4$ recorded at room temperature. All the compounds showed 3 bands in the Fe–O stretching region, suggesting a low symmetry of FeO_6 octahedra [13]. The higher band (665–670 cm^{-1}) was assigned to the Fe–O stretching frequency while the peak at lower frequency (330–365 cm^{-1}) is due to the deformation mode. The additional band at 525–570 cm^{-1} was assigned to the Ln–O stretching frequency. Singh and Ganguly [14] compared the IR spectra of oxides having K_2NiF_4 structure with pervoskite oxides. The highest frequency band, corresponding to the B–O bridge stretching frequency of $LnSrFeO_4$, was found to be higher than the B–O stretching frequency which appears at 540–560 cm^{-1} in $LnFeO_3$ oxides [12]. This was attributed to the difference in lattice parameters.

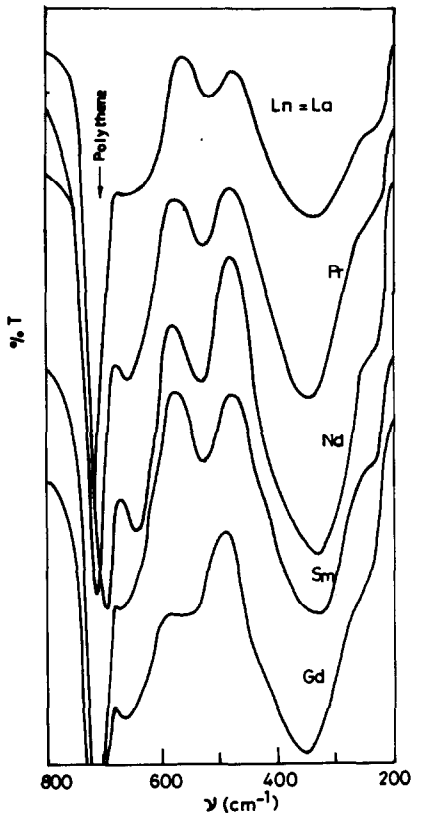

Fig. 1. IR spectra of $LnSrFeO_4$.

TABLE 2

Solid state properties of $LnSrFeO_4$

Compound	Sign of α	Electrical behaviour at 30 °C (Ω^{-1} cm^{-1})	Moment μ_{eff} (B. M.)	Surface area (m^2 g^{-1})
$LaSrFeO_4$	+	p-type semiconductor (1.4×10^{-4})	3.49	0.7
$PrSrFeO_4$	+	1.6×10^{-4}	4.31	1.0
$NdSrFeO_4$	+	3.5×10^{-5}	4.63	1.2
$SmSrFeO_4$	+	1.0×10^{-4}	3.55	1.0
$GdSrFeO_4$	+	2.8×10^{-5}	8.25	0.8

All the compounds in the series exhibit semiconducting behaviour. The positive Seebeck values (Table 2) indicate that holes are the majority charge carriers which are responsible for conduction. This confirms the fact that native defects play a major role in the conduction process. The conduction may be due to the hopping of positive holes from one site to the other among the localised levels. The high resistivity at room temperature observed in $LnSrFeO_4$ compared to $LnFeO_3$ [16] may be due to the presence of SrO layers between ABO_3 layers.

The magnetic moments calculated for $LnSrFeO_4$ are presented in Table 2. All the compounds are paramagnetic at room temperature. The magnitude of the magnetic moment (μ_{eff}) increases from La → Gd, indicating the participation of the rare earth in determining magnetic properties.

Surface characterisation

Characterisation of the surface of the catalyst is important because reactions take place on the catalyst surface. In the present investigation, the surface of $LnSrFeO_4$ was analysed by XPS to estimate the valence state of various elements and their relative surface concentrations. The C 1s peak at 285.0 eV was taken as the reference peak.

The salient features of XP spectra of $LnSrFeO_4$ are summarised in Table 3 and the spectra of Ln 3d, Fe 2p and O 1s regions are shown in Figs. 2–4. Figure 2 show the 3d level of Ln in $LnSrFeO_4$. In all the compounds, the rare earth is found to be in the trivalent state, as evidenced from binding energy values reported for corresponding rare earth oxides [17–19]. Rare earth oxides generally show satellite features (indicated by an arrow) which was considered to be due to charge transfer from O(2p) → metal (4f). In the case of La, the satellite is attributed to an energy loss process [20] and hence the satellite appears at a higher binding energy. In the case of other $LnSrFeO_4$ where Ln ≠ La, the satellite peaks appear at lower binding energies, which was attributed to the shake-down process [19].

XP spectra of the Ln 4d region, however, showed broad bands. The peculiar broad spectra of the 4d regions of the lanthanide ions were attributed

TABLE 3

XP spectral results[a] of $LnSrFeO_4$

Region	$LaSrFeO_4$		$PrSrFeO_4$		$NdSrFeO_4$		$SmSrFeO_4$		$GdSrFeO_4$	
	Core level	Satellite	Core level	Satellite	Core level	Satellite	Core level	Satellite	Core level	Satellite
O 1s	529.65		529.00		529.25		529.00		529.75	
	531.50		531.25		531.85		531.50		531.50	
Fe $2p_{3/2}$	710.75	718.00	710.75	717.75	710.50	718.25	710.50	718.25	711.00	717.0
$2p_{1/2}$	724.25		725.25		724.75		724.75		724.00	719.5
3p	55.25		55.75		56.00		55.75		55.50	
Ln $3d_{5/2}$	835.05	838.00	933.50	929.50	983.25	981.00	1084.50	1082.00	1187.00	1185.5
$3d_{3/2}$	852.50	855.10	953.25	950.50	1005.75	1003.00	1107.50	1105.00	1218.00	1215.5
4d	103.00		broad		broad		broad		broad	
	105.50									
Sr 3d	133.50		134.00		133.75		134.25		134.25	
	135.25		135.75		136.00		136.25		135.75	
2p	268.75		269.00		268.50		269.75		269.75	

[a]Binding energy in eV.

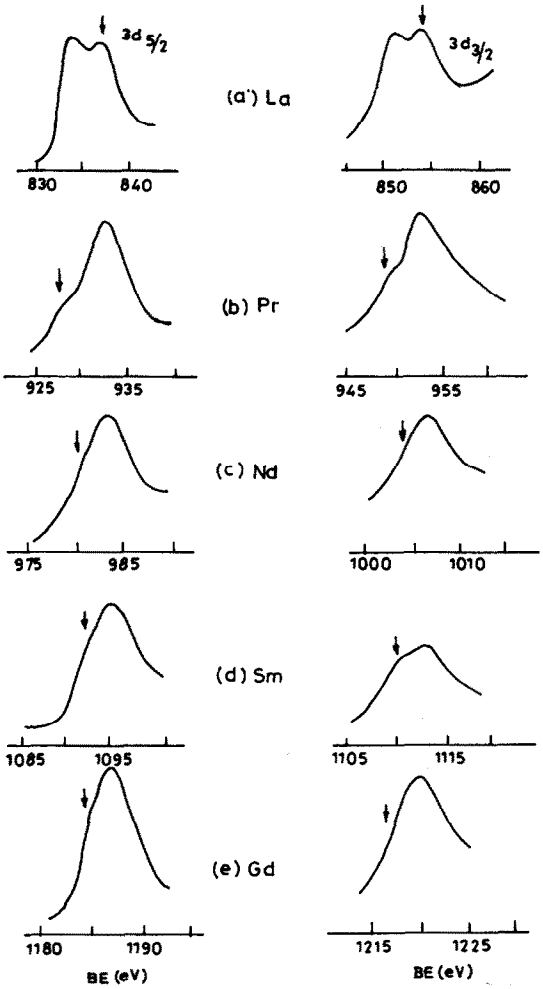

Fig. 2. XP (Ln 3d) spectra of $LnSrFeO_4$.

to electrostatic coupling between 4d and 4f, with concomitant production of many final states with different energies. The broad peaks may also be due to the fact that the 4d hole state has a very short lifetime [21]. However, La 4d showed sharp peaks due to the absence of electrons in the f-shell.

Figure 3 shows the Fe(2p) spectra of $LnSrFeO_4$ compounds. The binding energy values for Fe $2p_{3/2}$ for these compounds are found to be in the range 710–711 eV (Table 3), which clearly indicates the presence of iron in the trivalent state. This is in accordance with reports in the literature for Fe^{3+}-containing oxides [22–24]. However, $GdSrFeO_4$ showed a broad peak which might be due to the presence of iron in mixed valence states, namely Fe^{3+} and Fe^{2+}. The broad satellite peak centered between 717–719 eV (7–8 eV away from the Fe $2p_{3/2}$ peak) is characteristic of Fe^{3+} species, independent

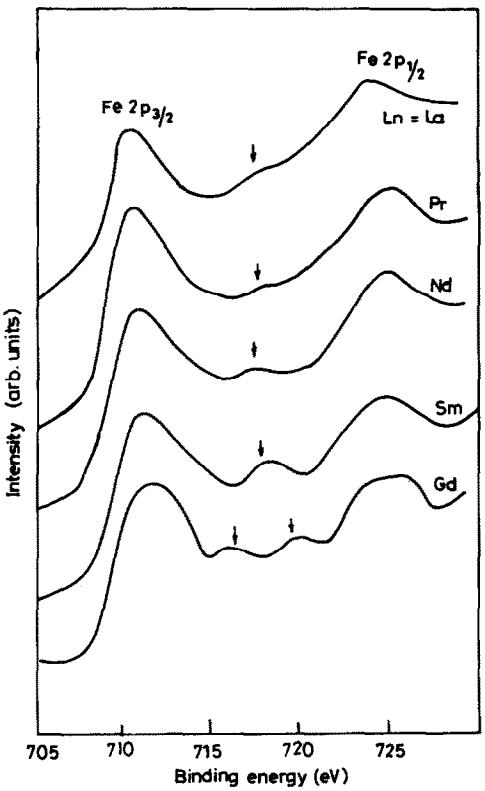

Fig. 3. XP (Fe 2p) spectra of $LnSrFeO_4$.

of the nature of the oxide and the coordination number [24]. The combination of the main $2p_{3/2}$ line and its satellite provides a reliable identification of the valence state of iron in these compounds. The presence of a satellite at ~717 eV in $GdSrFeO_4$ shows the possibility of a small amount of Fe^{2+} in the system along with Fe^{3+}. This is also evidenced from the broad peak for $2p_{3/2}$.

The XP(O 1s) spectra of $LnSrFeO_4$ are shown in Fig. 4. The spectra show two peaks, with binding energy values ~529 and ~531 eV respectively. These two peaks can be assigned to O^{2-} and O^-, OH^- or CO_3^{2-} species, as reported in literature [25, 26]. The XP(Sr 3d) spectra of $LnSrFeO_4$ show two peaks with binding energies ~133.5 and ~135.5 eV (Table 3), corresponding to $3d_{5/2}$ and $3d_{3/2}$, indicating the presence of strontium in the divalent state [27, 28].

Catalytic studies

The kinetic examination of N_2O decomposition was carried out on the series $LnSrFeO_4$ at two initial pressures of N_2O, namely 50 and 200 torr,

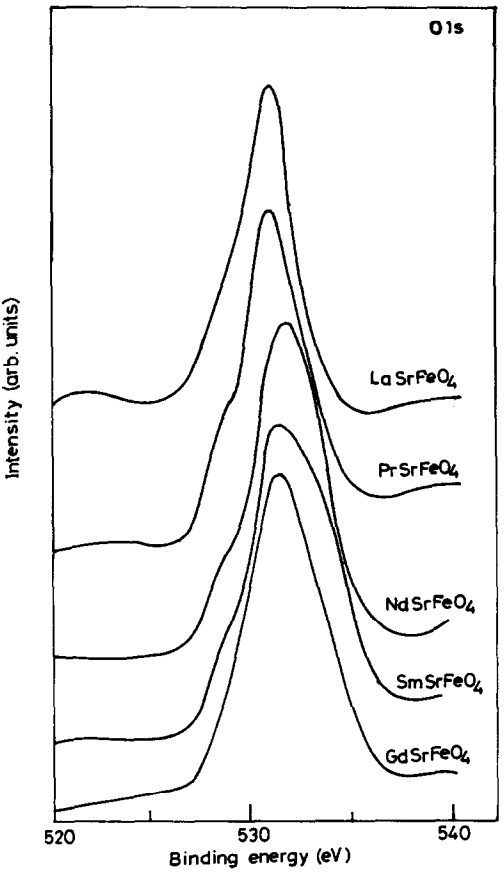

Fig. 4. XP (O 1s) spectra of $LnSrFeO_4$.

in the temperature range 400–480 °C. The kinetic results were analysed using the rate equations corresponding to no inhibition or strong inhibition [29].

$$dP_{N_2O}/dt = k_1 P_{N_2O} \quad \text{(I)}$$

$$dP_{N_2O}/dt = k_2 P_{N_2O}/P_{O_2}^{1/2} \quad \text{(II)}$$

Typical kinetic plots are shown in Fig. 5 and the corresponding kinetic parameters are presented in Tables 4 and 5. Using these rate constants, Arrhenius plots were drawn (Fig. 6) and the Arrhenius parameters are given in Tables 4 and 5.

At 50 torr, on all the catalysts, the kinetics obeyed the inhibition equation (I), indicating the adsorption of N_2O is rate controlling as shown below:

$$N_2O + e^- \longrightarrow N_2O^-_{ads} \quad (1)$$

$$N_2O^-_{ads} \longrightarrow N_2 + O^-_{ads} \quad (2)$$

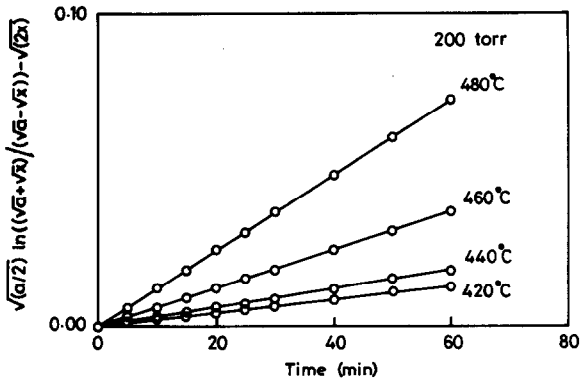

Fig. 5. Kinetic plots for the decomposition of N_2O on $LaSrFeO_4$.

TABLE 4

Kinetic and Arrhenius parameters for the decomposition of N_2O on $LnSrFeO_4$ at 50 torr[a]

Compound	Temp. (°C)	$k \times 10^3$ (min^{-1})	E_a (kcal mol^{-1})	ln A
$LaSrFeO_4$	440	0.91	32.8	16.0
	460	1.50		
	480	3.05		
$PrSrFeO_4$	420	2.72	24.0	11.4
	440	4.75		
	460	6.73		
	480	9.04		
$NdSrFeO_4$	420	0.96	23.8	10.0
	440	1.93		
	460	3.18		
	480	5.50		
$SmSrFeO_4$	440	1.23	28.6	13.4
	460	2.24		
	480	3.70		
$GdSrFeO_4$	420	2.18	1.71	6.6
	440	4.03		
	460	5.54		
	480	8.60		

[a]Kinetic equation obeyed: eqn. 1.10 (no inhibition).

$$O^-_{ads} + O^-_{ads} \longrightarrow O_2 + 2e^- \quad (3)$$

$$O^-_{ads} + N_2O \longrightarrow N_2 + O_2 + e^- \quad (4)$$

Generally at low pressure, N_2O adsorption occurs preferentially by the interaction of the π^* orbital of N_2O with the surface valence states of the oxide lattice. Because of the limited surface states, adsorption of N_2O becomes rate controlling. This is the case at 50 torr.

TABLE 5

Kinetic and Arrhenius parameters for the decomposition of N_2O on $LnSrFeO_4$ at 200 torr[a]

Compound	Temp. (°C)	$k \times 10^3$ ($mm^{1/2}$ min^{-1})	E_a (kcal mol^{-1})	ln A
$LaSrFeO_4$	420	0.21	37.5	20.5
	440	0.30		
	460	0.61		
	480	1.20		
$PrSrFeO_4$	400	2.47	30.0	14.9
	420	3.70		
	440	6.10		
	460	10.53		
$NdSrFeO_4$	400	1.15	35.2	11.9
	420	2.43		
	440	3.03		
	460	5.80		
$SmSrFeO_4$	420	1.10	31.3	16.8
	440	2.48		
	460	4.52		
	480	7.83		
$GdSrFeO_4$	400	3.51	18.7	8.2
	420	5.25		
	440	7.83		
	460	11.05		

[a]Kinetic equation obeyed: eqn. 1.11 (strong inhibition).

At high N_2O pressure, multipoint adsorption leads to population of the σ^* orbital of N_2O and hence causes facile N—O fission, resulting in a situation in which desorption of oxygen controls the overall rate due to the saturation with N_2O molecules. This is the case at 200 torr. The presence of a large density of filled localised electronic states of d-symmetry at the surface is essential for the adsorption of N_2O, while the localised empty d-orbitals are essential for oxygen desorption. In perovskite-related oxides, the d_{z^2} orbitals of B ions have the proper energy and symmetry to interact with N_2O molecules [30]. Thus the effect of pressure on the kinetics of decomposition is well portrayed in the present series. A similar effect of pressure on kinetics has been reported for perovskite oxides [31].

A linear correlation between the frequency factor and energy of activation at both pressures is shown in Fig. 7. These linear plots demonstrate that although the B site ions are responsible for their activity, the energetics of the B sites are modified significantly by the presence of different rare earth ions at the A sites and hence a compensation effect [32] was observed.

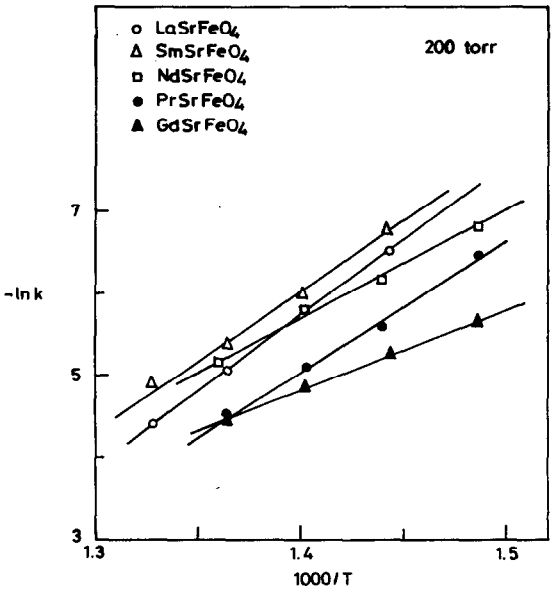

Fig. 6. Arrhenius plot for the decomposition of N_2O.

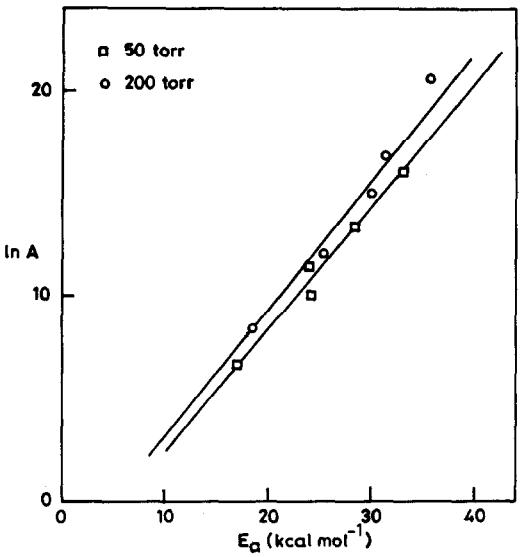

Fig. 7. Compensation plots.

Physicochemical correlations

Adsorption of N_2O in the multipoint mode has been well recognised on the mixed metal oxide catalysts [2, 4]. A similar model has been proposed for the adsorption of N_2O on $LnSrFeO_4$ catalysts. According to this model,

a molecular orbital scheme has been visualised for N_2O adsorption on clusters of the type M–O–M′ where M and M′ are different metal ions. In the present case, clusters of the type Ln–O–Fe, Ln–O–Sr, Sr–O–Fe, Ln–O–Ln and Fe–O–Fe are possible. In perovskite-related oxides, it is the B ion that plays the active role in deciding the solid state and catalytic properties, whereas the A ion plays only a modifying role. Therefore, when the A site ion is changed from La→Gd, the electron density around Fe is affected. In order to establish the role of the A ion in the catalytic decomposition of N_2O, which is the scope of the present investigation, the cluster of the type Ln–O– Fe is considered. Moreover, Sr^{2+} compounds are reported to be active only at very high temperature [33, 34].

The π^* orbital of N_2O has an orbital throw in a direction similar to the d_{z^2} orbitals of Fe^{3+}. The π orbital of middle nitrogen can interact with the p_z orbital of an oxide ion while π orbitals of a rare earth ion, having a maximum throw in the axial direction, lead to the multicentre adsorption of N_2O molecules, forming an adsorbed cluster over the Ln–O–Fe system.**

Recently Larsson [35] proposed another model for the adsorption of N_2O on clusters of the type M–O–M′ which is more appropriate than the former model. This model (Fig. 8) shows a schematic representation of the adsorption of N_2O on Ln–O–Fe clusters. During adsorption, the throw of orbitals in space is distorted due to the change in electron density around each atom. At a sufficient degree of activation, the N–O bond elongation is such that an $Fe^{3+}-O^-$ bond is formed. Further elongation leads to splitting of the N–O bond, giving rise to $N_2(g)$ and O^- on the surface.

The interaction between the axial f-orbitals of rare earth ions and the d_{z^2} orbital of iron with the p_z orbital of oxide ions depends on the electron density of the f-orbital of the rare earth ion. As the rare earth is changed from La→Gd, the f-electrons are filled successively, and the f–p_z interaction between the rare earth ion and the oxide ion of the lattice increases. Consequently the electron density around Fe^{3+} increases. As a result, the residual time of O^- on the iron site can be expected to decrease and desorption becomes facilitated. This is reflected in the decrease in E_a at 200

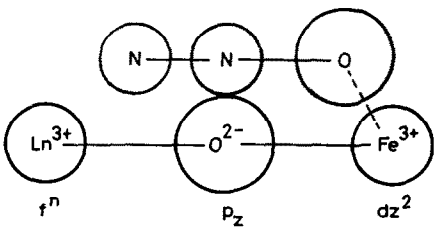

Fig. 8. Adsorption of N_2O on Ln–O–Fe cluster.

**The authors are thankful to the referee who pointed out that multipoint adsorption of N–N–O on Ln–O–Fe cluster is not possible based on bond length considerations.

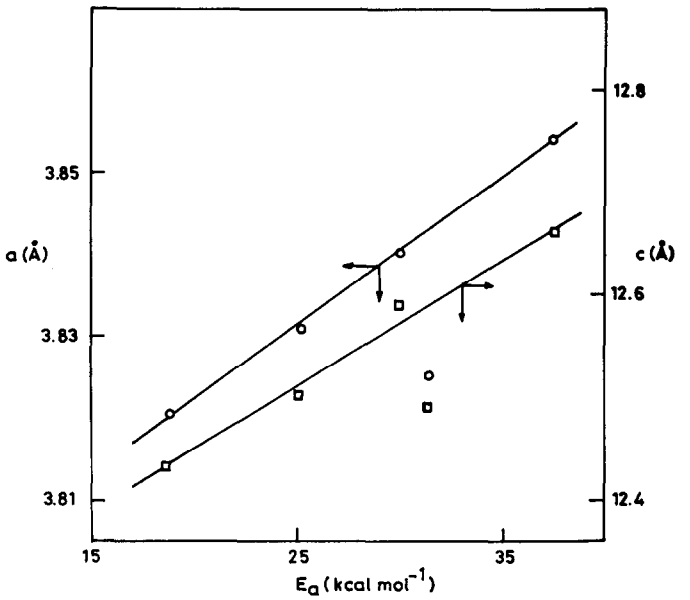

Fig. 9. Plot of E_a *vs.* lattice parameters.

torr from La → Gd, except Sm, on which at this pressure desorption of oxygen is rate controlling.

The plot of E_a *vs.* a or c presented in Fig. 9 shows a linear correlation between catalytic activity and lattice parameters. When the lattice parameter increases, the distance between two Fe^{3+} ions increases and makes the desorption process comparatively difficult, as it involves union of two O^- ions for the desorption of oxygen. This is reflected in the increase in E_a at 200 torr going from Gd → La.

As discussed above, desorption of oxygen involves union of two O^- to give an O_2 molecule. This involves decoupling of spins of the $p\pi$ orbital electron of an oxygen atom to form O_2. This kind of decoupling will be facile on catalysts having a high magnetic moment, as evidenced from the plot of E_a *vs.* μ_{eff} shown in Fig. 10. As μ_{eff} increases, the desorption of O^- as O_2 becomes facile and hence E_a decreases.

Figure 11 shows a plot of E_a *vs.* concentration of iron on the surface of the series $LnSrFeO_4$, calculated by the method of Powell and Larson [36]. A parallelism observed between E_a and surface concentration of iron indicates that Fe is the active site for the decomposition of N_2O. This is in accord with the compensation effect (Fig. 7) observed for the series. Figure 11 indicates that Fe is the active site for these oxides, while Fig. 7 indicates that the energetics of the active site are modified by the presence of a rare earth at A site.

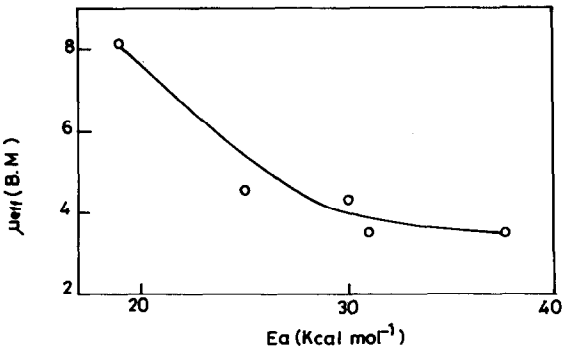

Fig. 10. Plot of E_a (200 torr) *vs.* μ_{eff}.

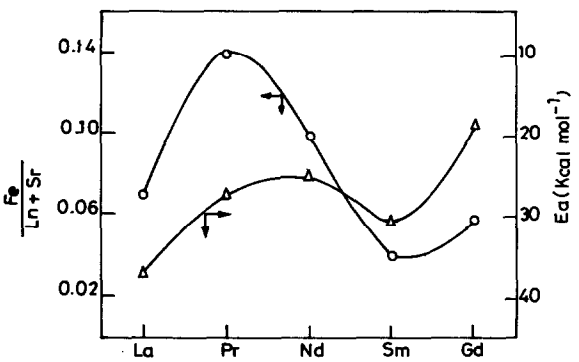

Fig. 11. Plot of E_a (200 torr) *vs.* concentration of Fe on the surface of $LnSrFeO_4$.

Acknowledgement

One of the authors (J.C.) thanks CSIR, New Delhi, for the financial assistance. The authors also thank RSIC, IIT Madras, for recording the XP spectra.

References

1 T. Nitadori, M. Muramatsu and M. Misono, *Bull. Chem. Soc. Jpn.*, *61* (1988) 3831.
2 K. V. Ramanujachary, K. M. Vijaya Kumar and C. S. Swamy, *React. Kinet. Catal. Lett.*, *20* (1982) 223.
3 L. R. LeCoustumer, Y. Barbaux, J. P. Bonnelle, J. Loriers and F. Clerc, *C.R. Acad. Sci., Paris, Ser. C, 290* (1980) 157.
4 K. V. Ramanujachary, N. Kameswari and C. S. Swamy, *J. Catal.*, *86* (1984) 121.
5 N. Gunasekaran, A. Meenakshisundaram and V. Srinivasan, *Surf. Technol.*, *22* (1984) 89.
6 N. Kameswari, J. Christopher and C. S. Swamy, *React. Kinet. Catal. Lett.*, *41* (1980) 381.
7 L. J. Tejuca, J. L. G. Fierro and J. M. D. Tascon, *Adv. Catal.*, *36* (1989) 237.
8 M. Shimada and M. Koizumi, *Mater. Res. Bull.*, *11* (1976) 1237.
9 G. Demazeau, Z. Li Ming, L. Fournes, M. Pouchard and P. Hagenmuller, *J. Solid State Chem.*, *72* (1988) 31.

10 B. Buffat, M. H. Tuilier, H. Dexpert, G. Demezeau and P. Hagenmuller, *J. Phys. Chem. Solids, 47* (1986) 491.
11 J. F. Ackerman, *Mater. Res. Bull., 14* (1979) 487.
12 G. Blasse, *J. Inorg. Nucl. Chem., 27* (1965) 2683.
13 P. Ganguly and C. N. R. Rao, *J. Solid State Chem., 53* (1984) 193.
14 K. K. Singh and P. Ganguly, *Spectrochim. Acta, 40 A* (1984) 539.
15 G. V. Subba Rao, C. N. R. Rao and J. R. Ferraro, *Appl. Spectrosc., 24* (1970) 436.
16 G. V. Subba Rao, B. M. Wanklyn and C. N. R. Rao, *J. Phys. Chem. Solids, 32* (1971) 345.
17 D. Briggs and M. P. Seah (eds.), *Practical Surface Analysis by Auger and X-ray Photoelectron Spectroscopy*, Wiley, New York, 1983.
18 J. C. Fuggle, H. Campagna, Z. Zolnierek, R. Lasser and A. Platau, *Phys. Rev. Lett., 45* (1980) 1597.
19 D. D. Sharma, P. Vishnukamath and C. N. R. Rao, *Chem. Phys., 73* (1983) 71.
20 P. Burroughs, A. Hammett, A. F. Orchard and G. Thronton, *J. Chem. Soc., Dalton Trans.*, (1976) 1686.
21 A. J. Signoralli and R. G. Hayes, *Phys. Rev., B 8* (1973) 81.
22 P. Selvam, B. Viswanathan, C. S. Swamy and V. Srinivasan, *Indian J. Technol., 25* (1987) 639.
23 C. R. Brundle, T. J. Chuang and K. Wandelt, *Surf. Sci., 68* (1977) 459.
24 L. Zhangola, C. Yun-gi and W. Xiao-Lin, *Surf. Sci., 147* (1984) 377.
25 M. S. Hedge and M. Ayyoob, *Surf. Sci., 173* (1986) L635.
26 P. Salvador, J. L. G. Fierro, J. Amadar, C. Cascales and I. Resines, *J. Solid State Chem., 81* (1989) 240.
27 K. Tabata, I. Matsumoto and S. Kohiki, *J. Mater. Sci., 22* (1987) 1882.
28 H. Van Doveren and J. A. Th. Verhoeren, *J. Electron Spectrosc. Relat. Phenom., 21* (1980) 265.
29 A. Cimino, V. Indovina, F. Pepe and F. S. Stone, *Gazz. Chim. Ital., 103* (1973) 935.
30 R. J. H. Voorhoeve, J. P. Remeika and L. E. Trimple, lecture, New York Academy of Science, Section Catalysis, 1974.
31 V. R. Sastri, R. Pitchai and C. S. Swamy, *Indian J. Chem., 18 A* (1979) 213.
32 H. C. Conner Jr., *J. Catal., 78* (1982) 238.
33 B. Viswanathan, *Indian Chem. Manuf., October* (1980) 1.
34 J. Nunan, J. A. Cronin and J. Cunningham, *J. Chem. Soc., Faraday Trans. 1, 81* (1985) 2027.
35 R. Larsson, *Catal. Today, 4* (1989) 235.
36 C. J. Powell and P. E. Larson, *Appl. Surf. Sci., 1* (1978) 186.